

Amplified positive effects on air quality, health, and renewable energy under China's carbon neutral target

Received: 15 October 2022

Accepted: 18 March 2024

Published online: 29 April 2024

 Check for updates

Yue Qin ^{1,2,9}✉, Mi Zhou ^{3,9}, Yueting Hao⁴, Xin Huang ⁴✉, Dan Tong ⁵, Liangdian Huang ^{1,2}, Chuan Zhang ^{2,6}, Jing Cheng ⁷, Weiyi Gu ^{1,2}, Licheng Wang^{1,2}, Xiaojia He⁸, Derong Zhou⁴, Qi Chen ^{1,2}, Aijun Ding ⁴ & Tong Zhu ¹

China pledged to achieve carbon neutrality by 2060 to combat global climate change, yet the resulting multi-aspect domestic impacts are not fully analysed due to an incomplete understanding of the underlying anthropogenic–natural interactions. Building an integrated cross-disciplinary modelling framework that can capture the feedbacks of changing aerosols on meteorology, here we highlight the amplified air quality, human health and renewable energy self-reinforcing synergies of China's carbon neutral target in comparison to the baseline in 2015 and 2060. We find that owing to emissions reduction and more favourable meteorological conditions caused by less aerosol, achieving China's carbon neutrality target in 2060 reduces national population-weighted PM_{2.5} concentrations and associated premature deaths by $-39 \mu\text{g m}^{-3}$ and 1.13 (95% confidence interval: 0.97–1.29) million while boosting provincial solar (wind) power performance by up to -10% (-6%) with mostly decreased resource variability in comparison to the 2060 baseline. Enhanced renewable performance along with low-carbon energy transition may provide additional opportunities to address the remaining air pollution and associated human health damages upon achieving carbon neutrality. Our results highlight that global developing and polluting countries' pledge for carbon neutrality can produce important positive feedbacks between aerosols mitigation, air quality improvement and enhanced renewable energy, which can be amplified via weakened aerosol–meteorology interactions and better atmospheric dispersion.

In light of increasing concerns about combating climate change, China's top government official pledged to peak national carbon dioxide emissions before 2030 and to be carbon neutral by 2060. Such an ambitious quest for carbon neutrality requires a profound domestic energy

structure transformation. For instance, the share of non-fossil energy in China's primary energy mix may need to increase from less than 16% in 2020 to over 80% by 2060^{1,2}, with solar and wind energy estimated to make up almost 37% and 36.5% of the electricity generation mix in

A full list of affiliations appears at the end of the paper. ✉ e-mail: qinyue@pku.edu.cn; xinhuang@nju.edu.cn

2060³, up from merely 3% and 6% in 2020, respectively⁴. In contrast, coal share is expected to drop from 57% to around 10% in the coming four decades^{5,6}.

Progressive energy (for example, renewables and/or natural gas) substitution for coal towards carbon mitigation can simultaneously reduce considerable air pollutant emissions, hence bringing remarkable air quality and associated human health co-benefits^{7–11}. Although the air quality co-benefits of low-carbon energy policies have been extensively evaluated^{12–15}, academic efforts have been started only recently to explore the potential air quality (and human health to a much lesser degree) synergies of China's carbon neutral target^{5,16–18}. In addition to emissions intensity, meteorology also plays a vital role in near-surface air pollution via atmospheric dispersion and diffusion, whereas atmospheric aerosols would substantially perturb the meteorological conditions directly through scattering and absorbing solar radiation (aerosol–radiation interactions (ARI)) and indirectly by modifying microphysical properties of clouds¹⁹. Specifically, those radiatively active aerosols, particularly light-absorbing black carbon, have been well proven to greatly deteriorate atmospheric dispersion conditions by warming the upper air and blocking sunlight that would otherwise warm the surface^{20–22}. The atmospheric heating and surface dimming induced by aerosols make the air increasingly stagnant, thereby greatly weakening air pollutants dilution²³. However, because most existing studies use either meteorology–chemistry decoupled (for example, WRF-CAMx) or reduced-form (for example, CHEER-AIR) regional air quality models, the underlying self-reinforcing feedback mechanisms and the amplifying air quality and human health benefits due to weakened aerosol–meteorology interactions under China's carbon neutral target have not been fully analysed^{5,16–18,24}.

Unlike the more frequently recognized air quality and human health co-benefits along with renewables penetration-induced carbon mitigation^{5,16,17,25}, improved wind–solar power performance under China's carbon neutral target has been much less analysed. As explained above, existing meteorology–chemistry decoupled integrated assessment frameworks are incapable of capturing the feedbacks of aerosols mitigation on meteorology and hence on solar and wind resource potential. Therefore, current related studies primarily rely on historical observational data to build statistic correlations between solar radiation and air pollution across China^{26–30}. Sweerts et al. (2019)²⁹ estimated solar energy losses owing to China's air pollution based on historical surface radiation data for the periods of 2003–2014 and 1960–2016, respectively. Similarly, using top-of-atmosphere insolation and aerosol optical depth reanalysis data, Chen et al. (2022)³⁰ identified the major drivers of interannual variations in solar potential for the period of 1995–2019 and discussed the possible implications for realizing China's 2060 carbon neutral target. Despite the valuable insights from existing literature, current history-oriented statistical studies cannot fully characterize the self-reinforcing feedbacks or unravel the underlying atmospheric physics and chemistry mechanisms between low-carbon energy transition and improved renewable energy performance in the context of China's carbon neutral pursuit.

Therefore, a systematic investigation of aerosols mitigation-induced positive feedback amplification between air pollution reduction, human health and renewable energy performance enhancement due to China's quest for carbon neutrality is largely missing, hindering a more comprehensive understanding of the multi-aspect impacts, interactions and hence potential local motivations to pursue carbon neutrality in countries facing dual challenges of domestic air pollution and global climate change.

Here we integrate China's carbon neutrality pathways developed from the GCAM-China (China-focused Global Change Assessment Model) and DPEC (Dynamic Projection for Emission in China) model, a meteorology–chemistry online coupled air quality model (WRF-Chem) and the Global Exposure Mortality Model (GEMM) to systematically evaluate the air quality, human health and renewable

energy performance synergies from China's ambitious target of achieving carbon neutrality by 2060. WRF-Chem model is used in this study because, unlike most other widely used air quality models (for example, GEOS-Chem), it is capable of capturing the feedbacks of changing aerosols on meteorology^{31,32}, hence allowing us to assess future wind and solar performance responses to achieving carbon neutrality, together with the air quality and associated human health impacts, and the underlying physical mechanisms (Extended Data Table 1). More analytical details are described in Methods.

Aerosols' impacts on air quality and renewable energy

By resolving high spatio-temporal resolution details of primary air pollutant emissions, local meteorology and chemical mechanisms, our simulations reveal considerable spatial heterogeneities in changing solar radiation, wind speed and near-surface PM_{2.5} (particles at or less than 2.5 μm in diameter) concentrations between with and without (w/o) considering aerosols' radiative effects (Fig. 1). The baseline simulation is validated using nationwide air quality monitoring data (Supplementary Fig. 1), which show a reasonably good model performance in capturing the spatial pattern and temporal variations in PM_{2.5}. Under the 2015 baseline, China has been suffering from high aerosol concentrations in both human emissions-intensive city clusters in eastern China and the dust source region in northwestern China.

High-loading aerosols covering China attenuate the solar energy that is supposed to heat the surface via absorbing and scattering solar radiation³³. The radiative effects of atmospheric aerosols are estimated to reduce annual mean solar radiation reaching the ground surface by approximately 11 W m^{-2} . In highly polluted regions such as the North China Plain and the Yangtze River Delta, grid-level reduction can reach over 35 W m^{-2} , resulting in up to 15% of local solar energy density losses. Reduced solar radiation reaching the ground surface due to aerosol extinction could further lead to a substantial drop in the convective motion and thus planetary boundary layer height, which is vital for the vertical dispersion and dilution of air pollutants (Supplementary Fig. 2). The atmospheric heating by light-absorbing aerosols, such as black carbon, further compound the stagnant air conditions and cause a lower planetary boundary layer height by forming a temperature inversion. Worse still, the weakened vertical exchange consequently leads to a lower near-surface wind speed with less downward momentum transfer (Fig. 1). Under a more unfavourable atmospheric dispersion and ventilation condition, air pollutants emitted near the surface tend to be accumulated in a much shallower boundary layer, rising national area-weighted (A-W) PM_{2.5} surface concentrations by 0.85 $\mu\text{g m}^{-3}$, even as high as 2.1 $\mu\text{g m}^{-3}$ for population-weighted (P-W) concentrations. In highly polluted and densely populated regions (for example, Beijing–Tianjin–Hebei and Sichuan–Chongqing), increment in provincial-level P-W PM_{2.5} surface concentrations are generally around 4 $\mu\text{g m}^{-3}$ (Extended Data Fig. 1), which may consequently result in considerable health damages. Notably, aerosol-induced solar radiation declines demonstrate a similar spatial pattern as that of PM_{2.5} concentrations, with provincial solar radiation reductions generally exceeding 15 W m^{-2} (>6%) across China's energy demand centres (Fig. 1 and Extended Data Fig. 2). In comparison, wind speed changes demonstrate a clearly different spatial pattern and are much smaller than solar radiation changes. Grid-level wind speed and hence resource performance can either increase or decrease due to aerosols' radiative effects, though it is dominated by decreasing trends in polluted regions due to weakened vertical flux of momentum.

We thereby highlight that the underlying aerosols' radiative effects would not only result in notable air quality degradation but also aggravate the geospatial mismatch between national energy supply and demand due to predominant aerosol-driven reductions in solar and wind resources across China's energy demand centres. Such aerosols' radiative effects would therein provide critical targeted opportunities

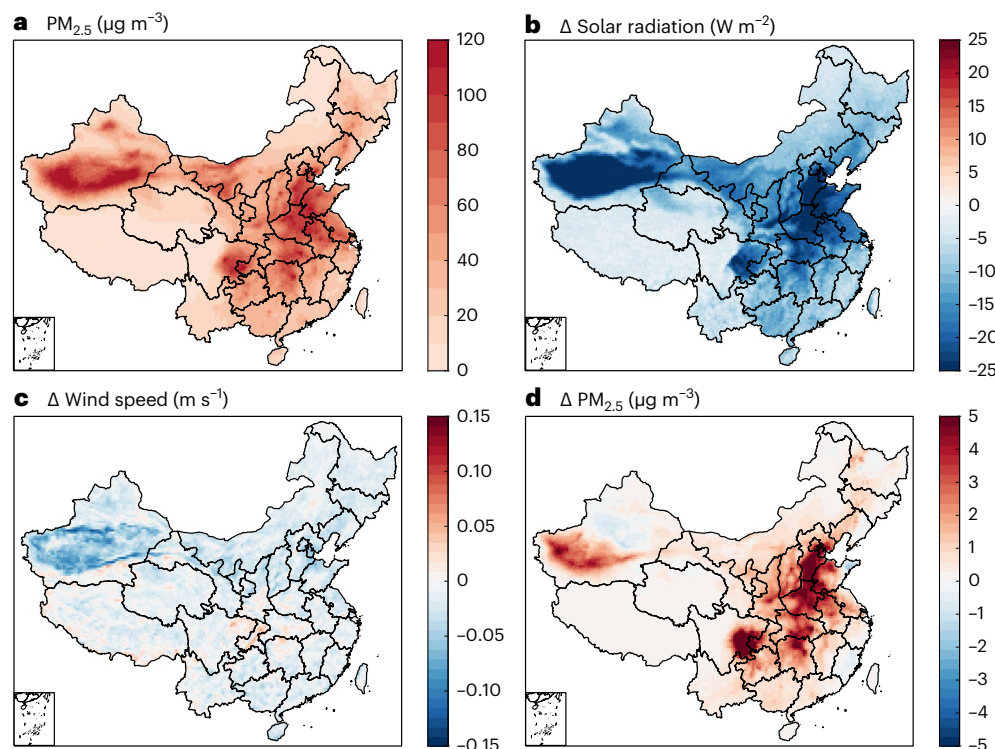


Fig. 1 | Aerosol distribution and its radiative effects on solar radiation, wind speed and air quality changes in 2015. a–d, Simulated annual mean $\text{PM}_{2.5}$ surface concentrations in China (a) and changes in solar radiation (b), wind speed (c) and $\text{PM}_{2.5}$ surface concentrations (d) in comparison to the hypothetical

case of no aerosols' radiative effects. Basemap data from the Resource and Environment Science and Data Center, Institute of Geographic Sciences and Natural Resources Research, Chinese Academy of Sciences (<https://doi.org/10.12078/2023010103>)³⁷.

to simultaneously improve local air quality and enhance renewable energy performance along with China's pursuit of carbon neutrality.

Amplified air quality and health under carbon neutrality

Increasing renewable substitution for fossil fuels under carbon neutrality brings progressive air pollutant emissions mitigation (Supplementary Fig. 3), causing notable $\text{PM}_{2.5}$ surface concentration reductions and avoided premature deaths in comparison to the 2060 baseline: $-14.6 \mu\text{g m}^{-3}$ and strikingly over $-38.8 \mu\text{g m}^{-3}$ of A-W and P-W $\text{PM}_{2.5}$ surface concentration reductions, respectively (Fig. 2, Extended Data Fig. 3, Supplementary Fig. 4 and Supplementary Table 1).

Such a prominent drop of $\text{PM}_{2.5}$ concentration not only results from direct emissions reduction but also a more favourable dispersion condition. Quantitatively, planetary boundary layer height and ventilation coefficient in eastern China could be increased by up to -7% and 6% , respectively, due to substantially weakened aerosol–meteorology interactions. In particular, aerosols' radiative effects alone can amplify $\text{PM}_{2.5}$ concentration reductions in Beijing, Tianjin and Hebei regions by 4.2 (5.4%), 4.7 (6.2%) and 2.8 (5.9%) $\mu\text{g m}^{-3}$ of A-W and 7.1 (6.5%), 5.6 (6.9%), 4.3 (6.6%) $\mu\text{g m}^{-3}$ of P-W, respectively, and 1.0 (6.5%) and 2.5 (6.3%) $\mu\text{g m}^{-3}$ of A-W together with 2.9 (7.5%) and 3.7 (7.4%) $\mu\text{g m}^{-3}$ of P-W $\text{PM}_{2.5}$ concentration reductions in Sichuan–Chongqing regions (Supplementary Fig. 5). Across the nation, ARI amplifies on average -0.5 and $1.5 \mu\text{g m}^{-3}$ of national A-W (3.8%) and P-W (4.0%) $\text{PM}_{2.5}$ concentration reductions, respectively. Greater reductions in national and regional P-W than A-W $\text{PM}_{2.5}$ concentrations highlight that air quality improvement resulting from China's quest for carbon neutrality predominantly occurs in areas with large population density, thereby bringing -1.13 (95% confidence interval: 0.97 – 1.29) million (-57%) reductions in $\text{PM}_{2.5}$ associated premature deaths in comparison to the 2060 baseline, among which ARI alone contributes $-23,000$ ($21,000$ – $26,000$)

reductions (Fig. 2, Extended Data Fig. 4, Supplementary Fig. 6 and Supplementary Table 2).

Without ambitious climate target and air pollution control, 780 million national population ($\sim 65\%$) in 2060 cannot meet China's current National Ambient Air Quality Standards (NAAQs) for annual average $\text{PM}_{2.5}$ concentrations ($35 \mu\text{g m}^{-3}$), with 8.9 million resulting from aerosols' radiative effect (Fig. 2 and Supplementary Fig. 7). However, when coupling carbon neutral climate policies with ambitious air pollution control (2060 Carbon neutral), except for 1.4% (17.8 million) of national population, almost the whole country can attain NAAQs. Thereby, carbon neutrality allows -760 million of the population to reach NAAQs, with -8.24 million contributed by reduced ARI effects. Likewise, China's carbon neutrality pledge decreases the proportion of the population exposed to air pollution above the World Health Organization (WHO)-10 and WHO-5 air quality guidelines by 42 and 0.9 percentage points, respectively, particularly across northern and central power grids.

Self-reinforcing renewable energy synergies

Carbon neutrality-oriented aerosols mitigation can not only improve local air quality but also enhance future solar and wind resources via perturbed earth–atmosphere energy balance, particularly in China's primary energy demand centres. Renewable energy enhancement will be increasingly beneficial in consort with rapidly growing solar and wind power penetration in China's energy mix as the country moves towards carbon neutrality.

As indicated in Fig. 3, we observe an almost consistent renewable power increase with decreasing hourly variability across the nation supposing achieving carbon neutrality in 2060 compared with lax climate and air pollution control due to enhanced solar radiation and wind speed (that is, 2060 Baseline; Supplementary Table 3). In particular, solar radiation increases generally exceed 6% across eastern provinces, while wind speed increases are much smaller (for example, up to -2%).

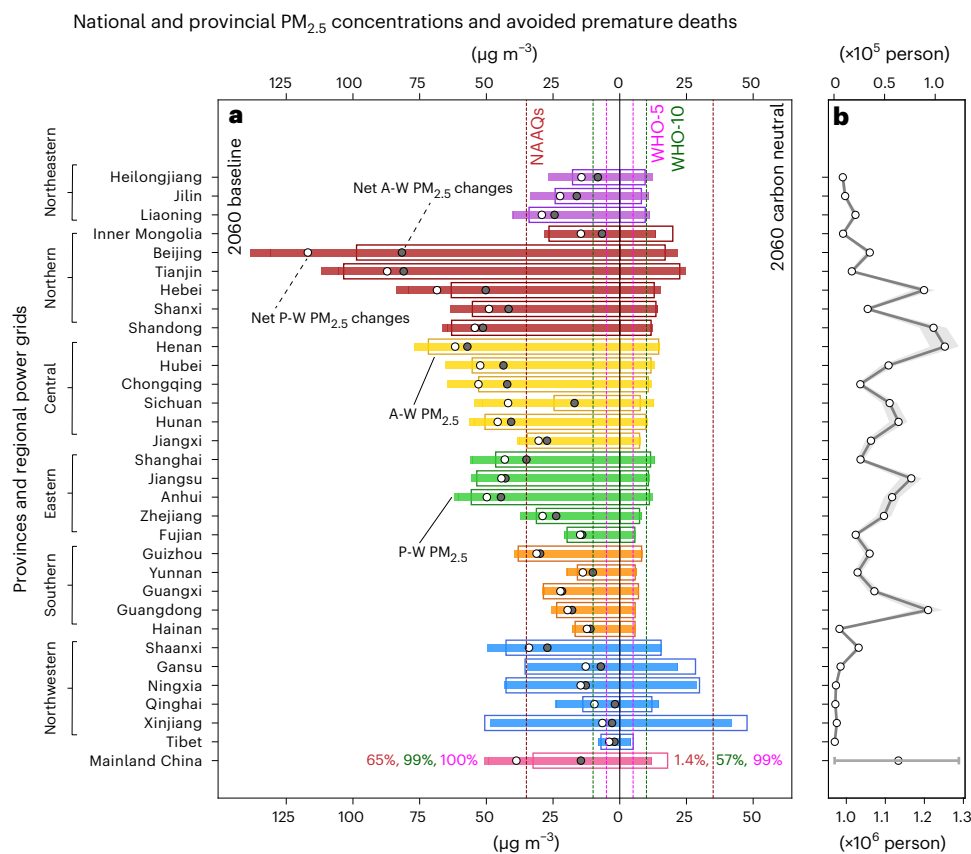


Fig. 2 | Air quality and human health co-benefits under China's carbon neutral target. a, Provincial P-W (coloured bars) and A-W (solid lines) PM_{2.5} surface concentrations in comparison to national (NAAQs, magenta dashed lines) and WHO air quality guidelines (WHO-10, green dashed lines; WHO-5, red dashed lines) under the 2060 baseline and 2060 carbon neutral scenarios across mainland China. Filled dots and open dots represent net changes in A-W and P-W PM_{2.5} concentrations between the 2060 carbon neutral and 2060 baseline

scenarios, respectively. Magenta, green and red numbers represent the national proportion of population exceeding NAAQs, WHO-10 and WHO-5, respectively. Provinces in different power grids are illustrated in different colours. **b**, Provincial avoided premature deaths, with the white dots representing the mean values and the grey shadow (error bands) and error bars representing the 2.5th and 97.5th percentiles ($n = 10,000$).

As a result, provincial solar power capacity factor (CF) increase is generally above 5% (up to 10%) with improving stability ($\Delta CV < -0.04$, coefficient of variability) in energy-demanding central, eastern and northern grids. In comparison, wind power increases upon achieving carbon neutrality are much less prominent, with the maximum provincial enhancement being around 6% and wind power variability can either increase or decrease. Across the country, central, southern and eastern grids demonstrate evident solar and wind performance enhancement with notable simultaneous CF increases and variability mitigation. Enhancing solar and wind resources in eastern provinces could thus potentially alleviate China's geospatial mismatch between energy demand and energy supply centres (Supplementary Fig. 8). Primarily due to strong interconnections between aerosols and solar radiation and associated vertical momentum, aerosols' feedbacks can notably enhance national solar and wind power CF by -2.6% (0.4 – 9.7% across provinces) and -0.6% (-0.1 – 5.7%), while increasing renewable resource stability, therein decreasing solar and wind CV by 1.2% (0.2 – 5.7%) and 0.4% (-0.9% to 1.7%), respectively.

Renewables to tackle the remaining environmental concerns

Due to aerosols' feedbacks, regions (for example, central and eastern grids) receiving substantial air quality benefits are often simultaneously experiencing notable renewable energy (solar, in particular) resource enhancement (Figs. 4 and 5), which are not only densely populated and heavily polluted but are also deeply energy demanding. That is, when achieving carbon neutrality, both air quality improvement

and renewable power enhancement occur in places where it is usually most needed.

That said, even achieving carbon neutrality in 2060 with progressive aerosol reduction and improved regional dispersion condition, 57% (724 million) and 99% (1.25 billion) of the national population are still exposed to air pollution above WHO-10 and WHO-5, respectively, among which 6.9 million and 1.2 million are ARI induced. Therefore, air pollution exposure under carbon neutrality can still lead to 0.84 (95% confidence interval: 0.70–0.98) million PM_{2.5} associated premature deaths, highlighting the value of further air quality improvement (Extended Data Fig. 4). As the low-carbon energy transition and associated aerosol reduction primarily take place across eastern provinces, China's carbon neutrality does not bring much air quality improvement within the northwestern grids (for example, Xinjiang and Gansu). These provinces thereby may end up turning to places with the worst air quality suffering from notable dust aerosols (Extended Data Fig. 3 and Supplementary Fig. 4). Meanwhile, the remaining PM_{2.5} associated premature deaths, upon realizing carbon neutrality, are still relatively high in eastern provinces, highlighting the value of air pollution control post-2060 (Extended Data Fig. 4). As air pollution mitigation potential from end-of-pipe controls are shrinking³⁴, progressive low-carbon energy transitions beyond carbon neutrality may provide additional air pollution mitigation opportunities, while simultaneously improving local renewable energy performance. This, however, is likely to be possible in consort with a breakthrough in energy storage technology in the next four decades. If so, enhanced solar and wind power performance from renewable-driven aerosol reduction can provide additional

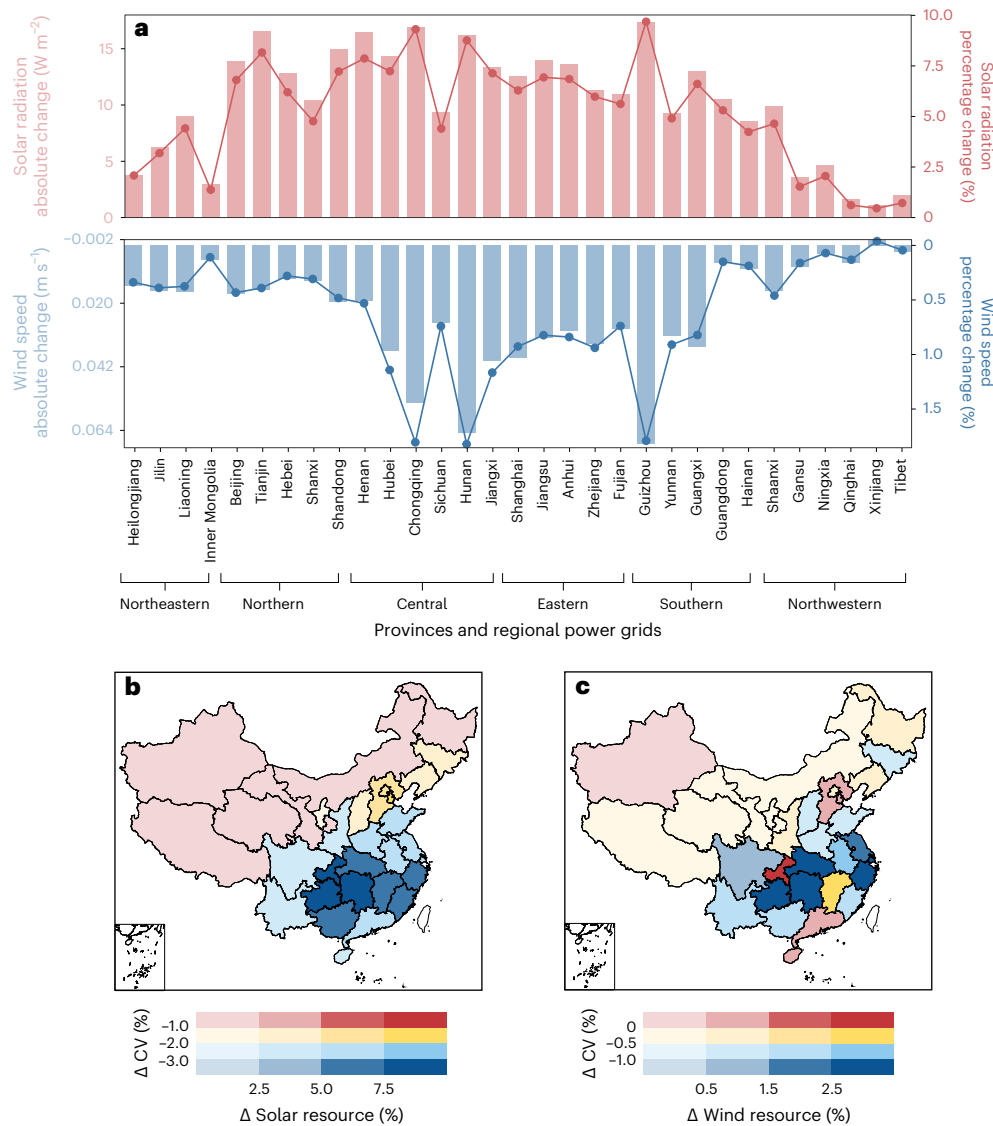


Fig. 3 | Renewable energy-related meteorology and performance changes under China's carbon neutral target. a, Provincial solar radiation (in red) and 10 m wind speed (in blue) absolute (bars) and percentage (lines) changes upon achieving carbon neutrality in comparison to the 2060 baseline across mainland China. Please note for wind speed changes, the axis is inverted (bottom positive, top negative). **b, c**, Corresponding changes in solar (**b**) and

wind power (**c**) performance represented by percentage changes in CF (x axis) and ΔCV (y axis). We generally find increasing resource performance and decreasing variability at the provincial level. Basemap data from the Resource and Environment Science and Data Center, Institute of Geographic Sciences and Natural Resources Research, Chinese Academy of Sciences (<https://doi.org/10.12078/2023010103>)³⁷.

local incentives for a more progressive low-carbon energy transition so as to further improve local air quality and reduce associated health damages post-carbon neutral, together with other non-fossil air pollution mitigation practices (for example, mitigation from industrial processes; Supplementary Fig. 9).

Discussion

Transforming China's fossil-dominated energy structure towards a low-carbon energy mix is widely considered as the cornerstone to achieving carbon neutrality, which could bring considerable air quality and human health co-benefits due to increasing renewables penetration in China's energy sector, while simultaneously enhancing renewable generation via aerosols reduction and hence weakened aerosol–meteorology interactions.

Integrating a renewable-driven carbon neutral roadmap with a regional meteorology–chemistry coupled air quality model, we find that due to both emissions reduction and aerosols reduction-induced better atmospheric dispersion, China's renewable energy penetration

under carbon neutrality will reduce national A-W $\text{PM}_{2.5}$ surface concentrations by $-14.6 \mu\text{g m}^{-3}$, thereby reducing population exposure by as high as $38.8 \mu\text{g m}^{-3}$ and avoiding 57% (–1.1 million, 95% confidence interval: 0.97–1.29 million) $\text{PM}_{2.5}$ associated premature deaths in comparison to lax climate and air pollution controls in 2060 (that is, 2060 Baseline), or reduce A-W and P-W $\text{PM}_{2.5}$ surface concentrations by $-16.9 \mu\text{g m}^{-3}$ and $-47.1 \mu\text{g m}^{-3}$, respectively, while avoiding 66% (–1.6 million, 95% confidence interval: 1.38–1.83 million) premature deaths in comparison to 2015 baseline. Ageing populations will often completely offset the health benefits from China's carbon neutrality target, though it could be fully compensated by reduced baseline mortality rate (Supplementary Fig. 10). Meanwhile, decreasing aerosols will perturb the earth–atmosphere balance and lead to increasing solar radiation (for example, over 6% across eastern provinces and a national average increase of –3%) and strengthened vertical flux of momentum (for example, up to 2% increases in wind speed with a national average increase of 0.3%), resulting in increasing solar and wind power CF with decreasing variability.

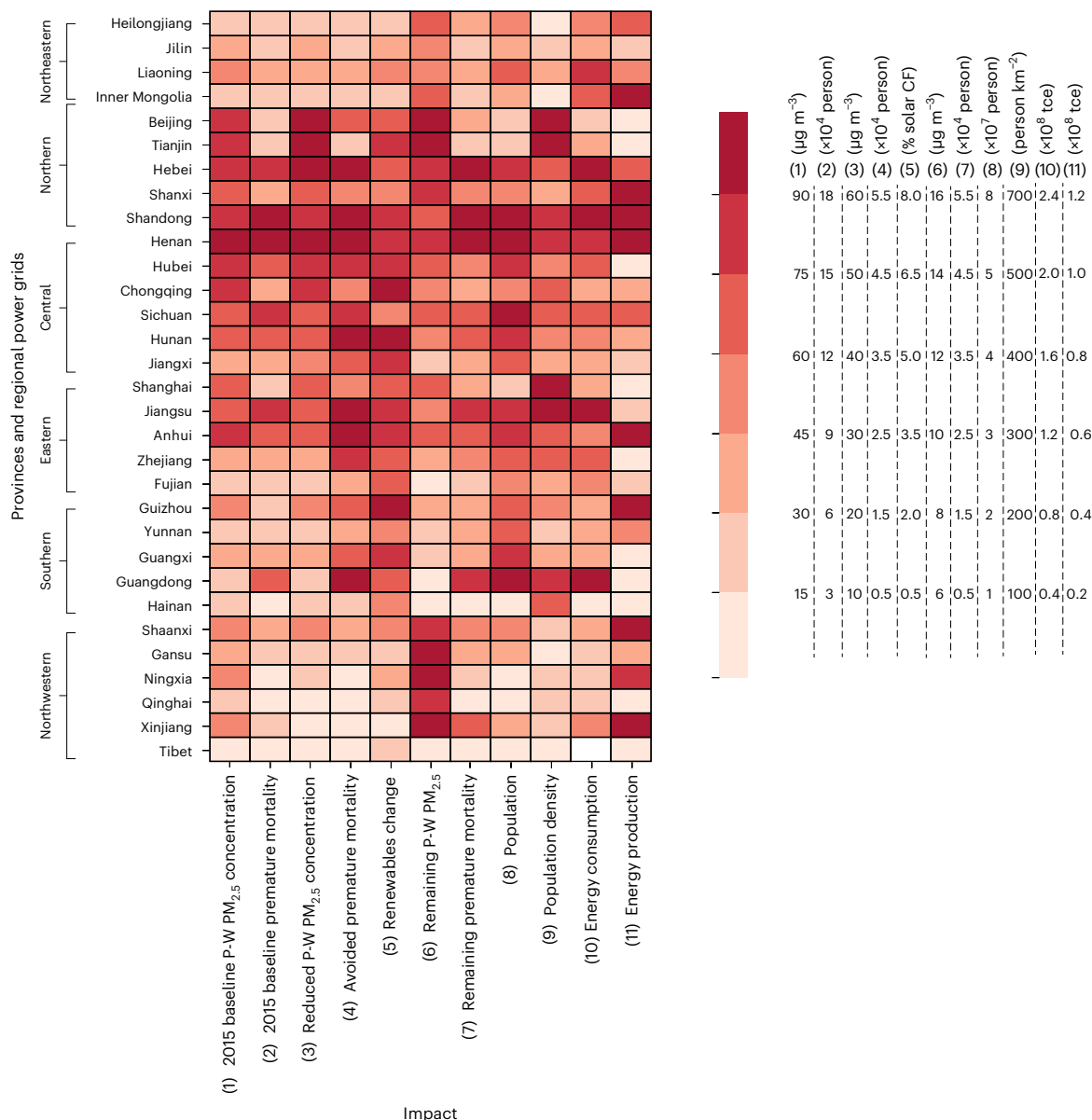


Fig. 4 | Multi-aspect synergies and self-reinforcing renewables under China's quest for carbon neutrality. Changes in provincial PM_{2.5} concentrations, associated premature deaths and renewable performance of China's carbon neutral scenario in comparison to the 2060 baseline, together with the remaining multi-aspect air pollution and health impacts upon achieving the 2060 carbon neutral target. Carbon neutrality achievement cannot fully

address various environmental consequences; multi-aspect synergies and self-reinforcing renewables may provide additional local incentives for further air quality and human health improvement. (6) Remaining P-W PM_{2.5} and (7) Remaining premature mortality refer to a P-W PM_{2.5} surface concentration (6) and PM_{2.5} associated premature mortality upon achieving carbon neutrality (7), respectively. tce, tonne of standard coal equivalent.

Particularly, regions receiving the largest air quality, human health and renewable resource synergies are concentrated in central, northern and eastern power grids, where provincial air pollution and population exposure reductions are generally around 80% (>40 µg m⁻³), the corresponding provincial avoided premature deaths are mostly above 60% (~50,000) and the solar and wind power CF increases can reach up to 10% and 6%, respectively, with decreasing hourly variability. Substantially larger reductions in P-W than A-W PM_{2.5} surface concentrations upon achieving carbon neutrality and the predominant renewable resource increases in heavily energy-demanding eastern provinces highlight that China's carbon neutrality-induced air quality, human health and renewable energy synergies primarily occur in places where such improvements are most needed, therefore helping to alleviate the geospatial mismatch between energy demand and energy supply.

China's quest for carbon neutrality brings considerable multi-aspect synergies supported by progressive low-carbon energy transitions and amplified by weakened aerosol–meteorology interactions and improved atmospheric dispersion condition across eastern provinces. Yet, post-carbon neutral air quality (~12.1 µg m⁻³) is still beyond the most recent WHO air quality guidelines, with 57% and 99% of the population exposed to PM_{2.5} concentrations exceeding 10 and 5 µg m⁻³, respectively. Thus, carbon neutrality does not completely address all environmental concerns we evaluate here, and additional air pollution mitigation strategies may still be needed from the human health perspective. Post-carbon neutral renewables facilitation may provide additional air pollution mitigation opportunities, together with strategies such as continuous energy efficiency improvement and emissions mitigation from non-fossil sources. That said, we highlight substantial uncertainties surrounding political and public



Fig. 5 | Conceptual model of multi-aspect synergies and renewable self-reinforcing effects. Grey arrows indicate the linkages between renewables penetration, air quality, greenhouse gas emissions and renewable energy performance, primarily in eastern China. Red and green arrows show respective increase and decrease of each parameter. Dashed red arrows indicate generally weaker wind speed increases in comparison to solar radiation. Grey rings indicate the self-reinforcing renewables may provide additional incentives for post-carbon neutral renewable energy promotion to address the remaining air pollution, together with other air pollution mitigation practices (for example, efficiency improvement and emissions mitigation from industrial processes). Chinese map from the Resource and Environment Science and Data Center, Institute of Geographic Sciences and Natural Resources Research, Chinese Academy of Sciences (<https://doi.org/10.12078/2023010103>)³⁷. World map underneath sourced from Natural Earth (<https://www.naturalearthdata.com/>).

willingness worldwide to meet the stringent WHO air quality guidelines upon that time. Current $\text{PM}_{2.5}$ concentrations are mostly above $5 \mu\text{g m}^{-3}$ across global major cities, even in those most developed regions³⁵. By then, factors such as an increasing value of a statistical life³⁶, the cost of available air pollution control technologies and the maturity of energy storage technology that affects the true costs of additional low-carbon energy transformation, will jointly determine the cost-effectiveness of post-carbon neutral air pollution abatement. Along that line, increasing renewables potential (especially solar) with decreasing resource variability in consort with aerosols reduction may provide extra local incentives for a more progressive low-carbon energy transition.

Our study reveals that China's carbon neutrality pursuit can produce an important self-reinforcing feedback loop between increasing renewables substitution for fossil fuels, aerosols reduction and renewable energy performance enhancement, which is amplified by perturbed earth-atmosphere energy balance and improved atmospheric dispersion condition. Therefore, the multi-aspect air quality and human health synergies and self-reinforcing low-carbon energy development, can potentially provide important local incentives for global developing and polluting countries to progressively transform towards, and even beyond, carbon neutrality.

Online content

Any methods, additional references, Nature Portfolio reporting summaries, source data, extended data, supplementary information, acknowledgements, peer review information; details of author contributions and competing interests; and statements of data and code availability are available at <https://doi.org/10.1038/s41561-024-01425-1>.

References

1. China Statistical Yearbooks (NBSC, 2021).
2. Working Guidance for Carbon Dioxide Peaking and Carbon Neutrality in Full and Faithful Implementation of the New Development Philosophy (CPC Central Committee and the State Council, 2021); http://www.gov.cn/xinwen/2021-10/24/content_5644613.htm
3. Zhu, W. K., Wang, C. Y., Wang, L. S., Wu, X. H. & Yue, Q. Analysis of energy-saving and environmental benefits from power structure adjustment in China: a comparative study from 2020 to 2060. *Sustain. Prod. Consump.* **31**, 750–761 (2022).
4. Data Explorer (EMBER, 2024); <https://ember-climate.org/data/data-explorer/>
5. Cheng, J. et al. Pathways of China's $\text{PM}_{2.5}$ air quality 2015–2060 in the context of carbon neutrality. *Natl Sci. Rev.* **8**, nwab078 (2021).
6. International Energy Agency An Energy Sector Roadmap to Carbon Neutrality in China (IEA, 2021); <https://www.iea.org/reports/an-energy-sector-roadmap-to-carbon-neutrality-in-china>
7. Siler-Evans, K., Azevedo, I. L., Morgana, M. G. & Apt, J. Regional variations in the health, environmental, and climate benefits of wind and solar generation. *Proc. Natl Acad. Sci. USA* **110**, 11768–11773 (2013).
8. Yang, J. N., Li, X. Y., Peng, W., Wagner, F. & Mauzerall, D. L. Climate, air quality and human health benefits of various solar photovoltaic deployment scenarios in China in 2030. *Environ. Res. Lett.* **13**, 064002 (2018).
9. Boudri, J. C. et al. The potential contribution of renewable energy in air pollution abatement in China and India. *Energy Policy* **30**, 409–424 (2002).
10. Qin, Y. et al. Air quality, health, and climate implications of China's synthetic natural gas development. *Proc. Natl Acad. Sci. USA* **114**, 4887–4892 (2017).
11. Qin, Y. et al. Air quality-carbon-water synergies and trade-offs in China's natural gas industry. *Nat. Sustain.* **1**, 505–511 (2018).
12. Yang, J. Z., Zhao, Y., Cao, J. & Nielsen, C. P. Co-benefits of carbon and pollution control policies on air quality and health till 2030 in China. *Environ. Int.* **152**, 106482 (2021).
13. Zhang, S. & Chen, W. Y. Assessing the energy transition in China towards carbon neutrality with a probabilistic framework. *Nat. Commun.* **13**, 87 (2022).
14. Liu, J. Y. et al. Identifying trade-offs and co-benefits of climate policies in China to align policies with SDGs and achieve the 2 degrees C goal. *Environ. Res. Lett.* **14**, 124070 (2019).
15. Yang, X. & Teng, F. Air quality benefit of China's mitigation target to peak its emission by 2030. *Clim. Policy* **18**, 99–110 (2018).
16. Zhang, S. H. et al. Incorporating health co-benefits into technology pathways to achieve China's 2060 carbon neutrality goal: a modelling study. *Lancet Planet. Health* **5**, E808–E817 (2021).
17. Shi, X. R. et al. Air quality benefits of achieving carbon neutrality in China. *Sci. Total Environ.* **795**, 148784 (2021).
18. Xu, B. Y. et al. Impacts of regional emission reduction and global climate change on air quality and temperature to attain carbon neutrality in China. *Atmos. Res.* **279**, 106384 (2022).
19. IPCC *Climate Change 2021: The Physical Science Basis* (eds Masson-Delmotte, V. et al.) (Cambridge Univ. Press, 2021); <https://doi.org/10.1017/9781009157896>

20. Hong, C. P. et al. Weakening aerosol direct radiative effects mitigate climate penalty on Chinese air quality. *Nat. Clim. Change* **10**, 845–850 (2020).
21. Zhou, M. et al. The impact of aerosol-radiation interactions on the effectiveness of emission control measures. *Environ. Res. Lett.* **14**, 024002 (2019).
22. Ding, A. J. et al. Enhanced haze pollution by black carbon in megacities in China. *Geophys. Res. Lett.* **43**, 2873–2879 (2016).
23. Huang, X., Wang, Z. L. & Ding, A. J. Impact of aerosol–PBL interaction on haze pollution: multiyear observational evidences in North China. *Geophys. Res. Lett.* **45**, 8596–8603 (2018).
24. Cheng, J. et al. A synergistic approach to air pollution control and carbon neutrality in China can avoid millions of premature deaths annually by 2060. *One Earth* **6**, 978–989 (2023).
25. Liu, Y. et al. Role of climate goals and clean-air policies on reducing future air pollution deaths in China: a modelling study. *Lancet Planet. Health* **6**, E92–E99 (2022).
26. Xia, X. G., Chen, H. B., Li, Z. Q., Wang, P. C. & Wang, J. K. Significant reduction of surface solar irradiance induced by aerosols in a suburban region in northeastern China. *J. Geophys. Res.: Atmos.* **112**, D22S02 (2007).
27. Yang, X., Zhao, C. F., Zhou, L. J., Wang, Y. & Liu, X. H. Distinct impact of different types of aerosols on surface solar radiation in China. *J. Geophys. Res.: Atmos.* **121**, 6459–6471 (2016).
28. Li, Z. Q. et al. Aerosol optical properties and their radiative effects in northern China. *J. Geophys. Res.: Atmos.* **112**, D22S01 (2007).
29. Sweerts, B. et al. Estimation of losses in solar energy production from air pollution in China since 1960 using surface radiation data. *Nat. Energy* **4**, 657–663 (2019).
30. Shi Chen et al. Improved air quality in China can enhance solar-power performance and accelerate carbon-neutrality targets. *One Earth* **5**, 550–562 (2022).
31. Zhou, M. et al. Environmental benefits and household costs of clean heating options in northern China. *Nat. Sustain.* **5**, 329–338 (2022).
32. Qin, Y. et al. Environmental consequences of potential strategies for China to prepare for natural gas import disruptions. *Environ. Sci. Technol.* **56**, 1183–1193 (2022).
33. Huang, X. et al. Direct radiative effect by multicomponent aerosol over China. *J. Clim.* **28**, 3472–3495 (2015).
34. Xing, J. et al. The quest for improved air quality may push China to continue its CO₂ reduction beyond the Paris Commitment. *Proc. Natl Acad. Sci. USA* **117**, 29535–29542 (2020).
35. WHO Air Quality Database (WHO, 2022); <https://www.who.int/data/gho/data/themes/air-pollution/who-air-quality-database>
36. Kniesner, T. J. & Viscusi, W. K. The value of a statistical life. *Economics and Finance* <https://doi.org/10.1093/acrefore/9780190625979.013.138> (2019).
37. Xu, Xl. China's multi-year provincial administrative division boundary data. *The Resource and Environment Science and Data Center, Institute of Geographic Sciences and Natural Resources Research, Chinese Academy of Sciences* <https://doi.org/10.12078/2023010103> (2023).

Publisher's note Springer Nature remains neutral with regard to jurisdictional claims in published maps and institutional affiliations.

Springer Nature or its licensor (e.g. a society or other partner) holds exclusive rights to this article under a publishing agreement with the author(s) or other rightsholder(s); author self-archiving of the accepted manuscript version of this article is solely governed by the terms of such publishing agreement and applicable law.

© The Author(s), under exclusive licence to Springer Nature Limited 2024

¹College of Environmental Sciences and Engineering, Peking University, Beijing, China. ²Institute of Carbon Neutrality, Peking University, Beijing, China. ³Princeton School of Public and International Affairs, Princeton University, Princeton, NJ, USA. ⁴School of Atmospheric Sciences, Nanjing University, Nanjing, China. ⁵Department of Earth System Science, Tsinghua University, Beijing, China. ⁶Institute of Energy, Peking University, Beijing, China. ⁷Department of Earth System Science, University of California, Irvine, CA, USA. ⁸The Administrative Center for China's Agenda 21, Beijing, China. ⁹These authors contributed equally: Yue Qin, Mi Zhou. ✉e-mail: qinyue@pku.edu.cn; xinhuang@nju.edu.cn

Methods

Scenario design

Integrating China's carbon neutrality pathways, an online meteorology–chemistry coupling air quality model and the GEMM, our study quantifies and highlights considerable national air quality, human health and renewable energy performance synergies in China's quest for carbon neutrality.

We obtain Chinese baseline and carbon neutral emissions scenarios from the GCAM-China (China-focused Global Change Assessment Model) and DPEC (Dynamic Projection for Emission in China) model, developed in Chen et al. (2021)⁵ and Tong et al. (2020)³⁸. As described in earlier studies, GCAM-China is expanded on GCAM (that is, an integrated assessment model representing the dynamics of both human and earth system) with greater spatial resolution for China and is used to simulate province-specific energy consumption and energy mix under China's carbon neutrality goal. DPEC model is designed in Tong et al. (2020)³⁸ to integrate the energy system, socio-economic projection and emissions inventory, thus provides scenario-specific air pollutants and CO₂ emissions. Baseline scenarios are designed with lax climate and air pollution policy following a highly unequal and isolated socio-economic pathway (SSP4–RCP6.0 with no new clean air actions beyond 2015; SSP, Shared Socioeconomic Pathway; RCP, Representative Concentration Pathway), which provides the 2015 reference point for other scenarios (that is, 2015 Baseline). Aerosol can perturb the energy budget by directly scattering or absorbing solar radiation^{39,40}, which can further result in a notable drop in convection, lower near-surface wind speed and unfavourable air pollution dispersion condition and hence further rise near-surface PM_{2.5} concentrations. Multiple studies have demonstrated that higher ambient PM_{2.5} concentrations directly lead to lower incident solar radiation^{27,30,39,40}, and Supplementary Fig. 15 illustrates a close link between PM_{2.5} concentrations and near-surface wind speed. We thereby also develop a counterfactual scenario that excludes aerosols' radiative effects (that is, 2015 Baseline-noARI) so as to explore the underlying mechanisms of how aerosols' radiative effects affect PM_{2.5} concentration reductions and renewable energy performance (that is, solar and wind power). The 2060 Baseline scenario is also designed to represent emissions changes under the business-as-usual pathway with (that is, 2060 Baseline) and without (that is, 2060 Baseline-noARI) including aerosols' radiative effects. Meanwhile, we have the scenario designed to pursue China's carbon neutral commitment with the best available end-of-pipe control technologies with (that is, 2060 Carbon neutral) and without (that is, 2060 Carbon neutral-noARI) including ARI (SSPI-China's net-zero CO₂ emissions in 2060) (Extended Data Table 1). Differences between with and without aerosols' radiative effects indicate ARI's amplifying effects, whereas differences between 2060 Baseline and 2060 Carbon neutral represent total effects of aerosols mitigation together with aerosols' feedbacks.

Online coupled regional meteorology–chemistry simulation

We further integrate emissions scenarios with the Weather Research and Forecasting model coupled with Chemistry (WRF-Chem) to simulate PM_{2.5} surface concentrations under each scenario. Unlike most other chemistry–meteorology decoupled atmospheric chemistry models used in integrated assessment frameworks, WRF-Chem model is capable of capturing the feedbacks of changing aerosols on meteorology (for example, solar radiation and wind speed) and hence on solar and wind power performance. The model has been widely used to reproduce air pollution and evaluate the radiative impacts of aerosols⁴¹. Some key physical parameterization options for the model are listed in Supplementary Table 4. For the chemical scheme, the Carbon-Bond Mechanism version Z photochemical mechanism and the four-bin version of the MOSAIC (Model for Simulating Aerosol Interactions and Chemistry) aerosol model are applied. Aerosols were assumed to be spherical particles. The sizes of aerosols were

divided into four discrete size bins defined by their lower and upper dry particle diameters. Aerosols in each size bin were assumed to be internally mixed. Aerosol optical properties were computed as a function of wavelength based on Mie theory. Aerosol's radiative effects were simulated using parameters including aerosol optical depth, single scattering albedo and asymmetry factor that were online estimated in the model⁴².

The WRF-Chem model domain, centred at (100.0° E, 37.0° N) with a 27 km × 27 km grid resolution, covers China and its surrounding areas (Supplementary Fig. 12). There were 37 vertical layers from the ground level to the top pressure of 50 hPa in which more than 16 layers were located below 2 km to well describe the vertical structure of the boundary layer. The simulation was conducted for January, April, July and October, with averaged results from these four seasons representing annual mean conditions. For simulations driven by the 2015 meteorology, the initial and boundary conditions of meteorological fields were updated from the 1-hour ERA5 (the fifth-generation atmospheric reanalysis of the European Centre for Medium-Range Weather Forecasts) data in 2015, with a 0.25° × 0.25° spatial resolution. For simulations driven by the 2060 meteorology, the initial and boundary meteorological conditions were derived from the downscaled and bias-corrected climate model simulations in 2060, with a 6-hour temporal resolution and a 1.25° × 1.25° spatial resolution⁴³ (Supplementary Fig. 13). Meteorological conditions are reinitiated every 48 hours to prevent drifting effects of the simulated meteorology⁴³. The chemical outputs from previous runs were used as the initial conditions for the following run. A similar modelling configuration and settings have been successfully adopted in our previous works³². Both natural and anthropogenic emissions were included for the regional WRF-Chem modelling in the present work. We applied the aforementioned DPEC dataset for characterizing anthropogenic emissions, in which emission sources were classified into five sectors: power plants, residential combustion, industrial process, on-road mobile sources and agricultural activities. The natural dust emissions were calculated online using Goddard Chemistry Aerosol Radiation and Transport (GOCART) module based on surface wind speed⁴⁴.

As illustrated in Supplementary Fig. 1, the baseline simulation is validated using nationwide air quality monitoring data, which show a reasonably good model performance in capturing the spatial pattern and temporal variations in PM_{2.5}. Spatial and temporal correlation of wind speed and solar radiation are validated against the ERA5 reanalysis data (Supplementary Figs. 14 and 15).

On the basis of simulated grid-level PM_{2.5} surface concentrations, we estimate provincial and national area-weighted ($C_{AW}(R) = \frac{\sum_{i=1}^n Area_i(R) \times C_i(R)}{\sum_{i=1}^n Area_i(R)}$) and population-weighted ($C_{PW}(R) = \frac{\sum_{i=1}^n Pop_i(R) \times C_i(R)}{\sum_{i=1}^n Pop_i(R)}$) PM_{2.5} surface concentrations in comparison to China's national air quality standards (NAAQs) (35 μg m⁻³), the previous (10 μg m⁻³) and recently updated (5 μg m⁻³) WHO air quality guidelines for annual average PM_{2.5} surface concentrations. $C_{AW}(R)$ and $C_{PW}(R)$ refer to national or provincial area-weighted and population-weighted PM_{2.5} surface concentrations in region R (province or the whole country), $Area_i(R)$ and $Pop_i(R)$ refer to grid area and population in each grid i within region R and $C_i(R)$ refers to model-simulated grid-level PM_{2.5} surface concentrations in grid i in region R . Population-weighted PM_{2.5} surface concentration (C_{PW}) is often referred to as population exposure. Supplementary Table 5 shows China's inter-provincial regional power grids⁴⁵.

Air pollution associated human health impacts evaluation

We then further quantify grid-level PM_{2.5}-associated premature mortality under each scenario using equations (1) and (2). We extract grid-level age-specific population for China in 2015 under different SSP scenarios from Wang and Sun (2022)⁴⁶ and retrieve national baseline mortality

rates from the Global Burden of Diseases study 2017 (<https://gbd2017.healthdata.org/gbd-search/>). We generate 10,000 shapes of relative risks (RR) and calculate the 95% confidence intervals of premature mortality under each scenario by perturbing the value of θ based on its mean and standard error described in Burnett et al. (2018)⁴⁷.

$$\text{Mort}_{j,i} = \text{POP}_{j,i,k} \times \text{Mortbase}_{j,k} * (1 - 1/\text{RR}_{j,i}) \quad (1)$$

where $\text{Mort}_{j,i}$ is the number of premature mortality in grid i from disease j , $\text{POP}_{j,i,k}$ is the number of exposed targeted population in grid i from disease j for adults' age group k (for example, 25–29), $\text{Mortbase}_{j,k}$ is the baseline mortality rate for respective adults group k for disease j , $\text{RR}_{j,i}$ is the relative risk for disease j in grid i . Here we use more recent GEMM developed in Burnett et al. (2018)⁴⁷, which covers the global range of exposures and is widely considered to be suitable for evaluating health impacts for China's high $\text{PM}_{2.5}$ concentrations. GEMM quantifies premature mortality for noncommunicable diseases and lower respiratory infections for adults (≥ 25 years old), with the threshold of no health effects at $2.4 \mu\text{g m}^{-3}$. Equation (2) below estimates the corresponding RR under GEMM. Supplementary Table 6 summarizes the parameters used in the GEMM model.

$$\text{RR}(z) = e^{\frac{\theta \times \log(\frac{z}{c} + 1)}{1 + e^{-\frac{\theta}{v}}}}, z = \max(0, c - 2.4) \quad (2)$$

In equation (2), c represents the long-term ambient $\text{PM}_{2.5}$ concentration; θ , μ and v represents parameters that determine the shape of RR in GEMM and are specified for each age group; e is natural logarithm; $2.4 \mu\text{g m}^{-3}$ is the threshold for $\text{PM}_{2.5}$, below which there will be no effect; and z is defined as the max value between 0 and $c - 2.4$.

In addition to GEMM, we use two other different health impacts models (GEMM-5 diseases and integrated exposure response (IER) functions) to evaluate human health impacts as sensitivity analysis. GEMM-5 diseases model is constructed in Burnett et al. (2018)⁴⁷ that includes the same five diseases as IER: ischaemic heart disease, stroke, chronic obstructive pulmonary disease, lung cancer and lower respiratory infections. Detailed parameters for GEMM-5 diseases are listed in Table S2 in Burnett et al. (2018)⁴⁷, and the same RR equation (equation (2)) is used for GEMM-5 diseases models. Disease-specific IER RRs are also obtained from the global burden of disease studies for age-specific population groups; then equation (1) is used to quantify disease-specific premature deaths. We further obtain the age distribution and baseline mortality rate changes in 2060 from earlier studies⁴⁸, with the respective age distribution and mortality rate under 2060 SSP4 used for the 2060 baseline scenario and under the 2060 SSP1 used for the 2060 carbon neutral scenario according to how these two scenarios are designed (Extended Data Table 1).

Solar and wind power performance evaluation

We calculate the capacity factor (CF) for solar power using scenario-specific outputs from the WRF-Chem model, applying the same method used in Jerez⁴⁹ and Feron⁵⁰ (equations (3)–(5)). All variables used and their corresponding units are listed in Supplementary Table 7. CF illustrates the performance of the photovoltaic cell under actual environmental conditions in comparison to rated power capacity. I and I_{STC} ($1,000 \text{ W m}^{-2}$) indicate downward shortwave radiation (W m^{-2}) under actual environmental conditions and standard test conditions, respectively; whereas P_R indicates the effects of actual temperature on the performance of photovoltaic panels. T_{cell} ($^{\circ}\text{C}$) is the cell temperature, T_{STC} is the cell temperature under standard test conditions (25°C) and γ equals $0.005^{\circ}\text{C}^{-1}$. T_{cell} relates to ambient temperature at 2 m (T_{2m} , $^{\circ}\text{C}$), downward shortwave radiation (I , W m^{-2}) and wind speed at 10 m (u_{10m} , m s^{-1}), where $c_1 = 4.3^{\circ}\text{C}$, $c_2 = 0.943$, $c_3 = 0.028^{\circ}\text{C} (\text{W m}^{-2})^{-1}$, $c_4 = 1.528^{\circ}\text{C} (\text{m s}^{-1})^{-1}$ (ref. 49).

In equations (3)–(5), the subscripts i, j, k denote the variable value at (i, j) position and at the hour k .

$$\text{CF}_{i,j,k} = P_{R_{i,j,k}} \left(\frac{I_{i,j,k}}{I_{\text{STC}}} \right) \quad (3)$$

$$P_{R_{i,j,k}} = 1 - \gamma(T_{\text{cell}_{i,j,k}} - T_{\text{STC}}) \quad (4)$$

$$T_{\text{cell}_{i,j,k}} = c_1 + c_2 T_{2m_{i,j,k}} + c_3 I_{i,j,k} - c_4 u_{10m_{i,j,k}} \quad (5)$$

Wind power CF is evaluated based on the atmospheric kinetic energy equation of the atmosphere and an idealized power curve for wind turbine using equations (6) and (7)⁵¹. Assuming the wind turbine hub height is of 100 m, the wind speed at 100 m (u_{100m}) is derived from wind speed at 10 m (u_{10m}) using the wind profile formula:

$$u_{100m} = u_{10m} \left(\frac{100}{10} \right)^{0.14} \quad (6)$$

Following earlier studies⁵², we assume the cut-in wind speed (u_{in}) is 3 m s^{-1} (below the cut-in speed the wind power turbine will not rotate), the cut-out wind speed (u_{out}) is 25 m s^{-1} (above the cut-out speed the wind power turbine will shut down for safety reasons), and the rated wind speed (u_{rated}) is 12 m s^{-1} ; hourly capacity factor is calculated by equation (7) (the meaning of i, j, k are the same as above):

$$\text{CF}_{i,j,k} = \begin{cases} 0 & (u_{100m_{i,j,k}} < u_{in} \text{ OR } u_{100m_{i,j,k}} > u_{out}) \\ \frac{u_{100m_{i,j,k}}^3 - u_{in}^3}{u_{rated}^3 - u_{in}^3} & (u_{in} \leq u_{100m_{i,j,k}} \leq u_{rated}) \\ 1 & (u_{rated} < u_{100m_{i,j,k}} \leq u_{out}) \end{cases} \quad (7)$$

We further use the coefficient of variation (CV) to quantify the hourly variability of solar and wind energy capacity factors. The hourly coefficient of variation is defined as the ratio of the hourly CF standard deviation to the hourly average CF in each month (equation (8))³⁰.

$$\text{CV} = \frac{\text{std}(\text{CF})}{\text{avg}(\text{CF})} \quad (8)$$

Data availability

Meteorology data for 2015 are obtained from the 1-hour ERA5 climate reanalysis dataset (<https://cds.climate.copernicus.eu/#!/search?text=ERA5&type=dataset>)⁵³; natural and anthropogenic fire emissions are from the Fire Inventory from NCAR (FINN; <https://www2.acom.ucar.edu/modeling/finn-fire-inventory-ncar>)⁵⁴; anthropogenic emissions are from the DPEC emissions inventory v1.1 (http://meicmodel.org.cn/?page_id=1918&lang=en)⁵⁵; 2060 meteorological data are available via figshare at <https://doi.org/10.6084/m9.figshare.16802326> (ref. 56). Source codes of the WRF-Chem model utilized in this study are available at <https://github.com/wrf-model/WRF/releases/tag/V3.6.1>. All source data generated or analysed during this study are included in this published paper (and its Supplementary Information) and are available at <https://doi.org/10.6084/m9.figshare.25302031> (ref. 57).

Code availability

The Python and R scripts for processing and plotting results in this study are available at <https://doi.org/10.6084/m9.figshare.25302031> (ref. 57).

References

38. Tong, D. et al. Dynamic projection of anthropogenic emissions in China: methodology and 2015–2050 emission pathways under a range of socio-economic, climate policy, and pollution control scenarios. *Atmos. Chemis. Phys.* **20**, 5729–5757 (2020).

39. Ramanathan, V., Crutzen, P. J., Kiehl, J. T. & Rosenfeld, D. Atmosphere–aerosols, climate, and the hydrological cycle. *Science* **294**, 2119–2124 (2001).
40. Hansen, J., Sato, M. & Ruedy, R. Radiative forcing and climate response. *J. Geophys. Res.: Atmos.* **102**, 6831–6864 (1997).
41. Huang, X. et al. Amplified transboundary transport of haze by aerosol-boundary layer interaction in China. *Nat. Geosci.* **13**, 428–434 (2020).
42. Chapman, E. G. et al. Coupling aerosol-cloud-radiative processes in the WRF-Chem model: investigating the radiative impact of elevated point sources. *Atmos. Chem. Phys.* **9**, 945–964 (2009).
43. Xu, Z. F., Han, Y., Tam, C. Y., Yang, Z. L. & Fu, C. B. Bias-corrected CMIP6 global dataset for dynamical downscaling of the historical and future climate (1979–2100). *Sci. Data* **8**, 293 (2021).
44. Ginoux, P. et al. Sources and distributions of dust aerosols simulated with the GOCART model. *J. Geophys. Res.: Atmos.* **106**, 20255–20273 (2001).
45. Zhou, X. X. et al. An overview of power transmission systems in China. *Energy* **35**, 4302–4312 (2010).
46. Wang, T. T. & Sun, F. B. Global gridded GDP data set consistent with the shared socioeconomic pathways. *Sci. Data* **9**, 221 (2022).
47. Burnett, R. et al. Global estimates of mortality associated with long-term exposure to outdoor fine particulate matter. *Proc. Natl Acad. Sci. USA* **115**, 9592–9597 (2018).
48. Yang, H., Huang, X. Y., Westervelt, D. M., Horowitz, L. & Peng, W. Socio-demographic factors shaping the future global health burden from air pollution. *Nat. Sustain.* **6**, 58–68 (2023).
49. Jerez, S. et al. The impact of climate change on photovoltaic power generation in Europe. *Nat. Commun.* **6**, 10014 (2015).
50. Feron, S., Cordero, R. R., Damiani, A. & Jackson, R. B. Climate change extremes and photovoltaic power output. *Nat. Sustain.* **4**, 270–276 (2021).
51. Pryor, S. C., Barthelmie, R. J., Bukovsky, M. S., Leung, L. R. & Sakaguchi, K. Climate change impacts on wind power generation. *Nat. Rev. Earth Environ.* **1**, 627–643 (2020).
52. Tong, D. et al. Geophysical constraints on the reliability of solar and wind power worldwide. *Nat. Commun.* **12**, 6146 (2021).
53. ERA5 climate reanalysis dataset. *Copernicus* <https://cds.climate.copernicus.eu/#!/search?text=ERA5&type=dataset> (2024).
54. FINN. NCAR <https://www2.acom.ucar.edu/modeling/finn-fire-inventory-ncar> (2024).
55. DPEC emission inventory. *MEICModel* http://meicmodel.org.cn/?page_id=1918&lang=en (2024).
56. Metadata record for: bias-corrected CMIP6 global dataset for dynamical downscaling of the historical and future climate (1979–2100). *figshare* <https://doi.org/10.6084/m9.figshare.16802326> (2021).
57. Qin, Y. Amplified positive environmental and energy effects under China' carbon neutrality. *figshare* <https://doi.org/10.6084/m9.figshare.25302031> (2024).

Acknowledgements

The work was financially supported by the National Natural Science Foundation of China grant number 42325506 to X. Huang, grant number 42277482 to Y.Q. and Fundamental Research Funds for the Central Universities (14380198) to A.D. M.Z. acknowledges support from the Princeton School of Public and International Affairs and its Center for Policy Research on Energy and the Environment. C.Z. acknowledges National Key R&D Program of China (grant number 2023YFF0613900). X. He acknowledges the Top-Notch Young Talents Program of China.

Author contributions

Y.Q. and X. Huang designed this study. X. Huang, M.Z., Y.Q., Y.H., D.T., L.H., C.Z., J.C., W.G., L.W., X. He, D.Z. and Q.C. led the model simulations and analysed the data. Y.Q., X. Huang, M.Z., A.D. and T.Z. wrote the paper with input from all co-authors.

Competing interests

The authors declare no competing interests.

Additional information

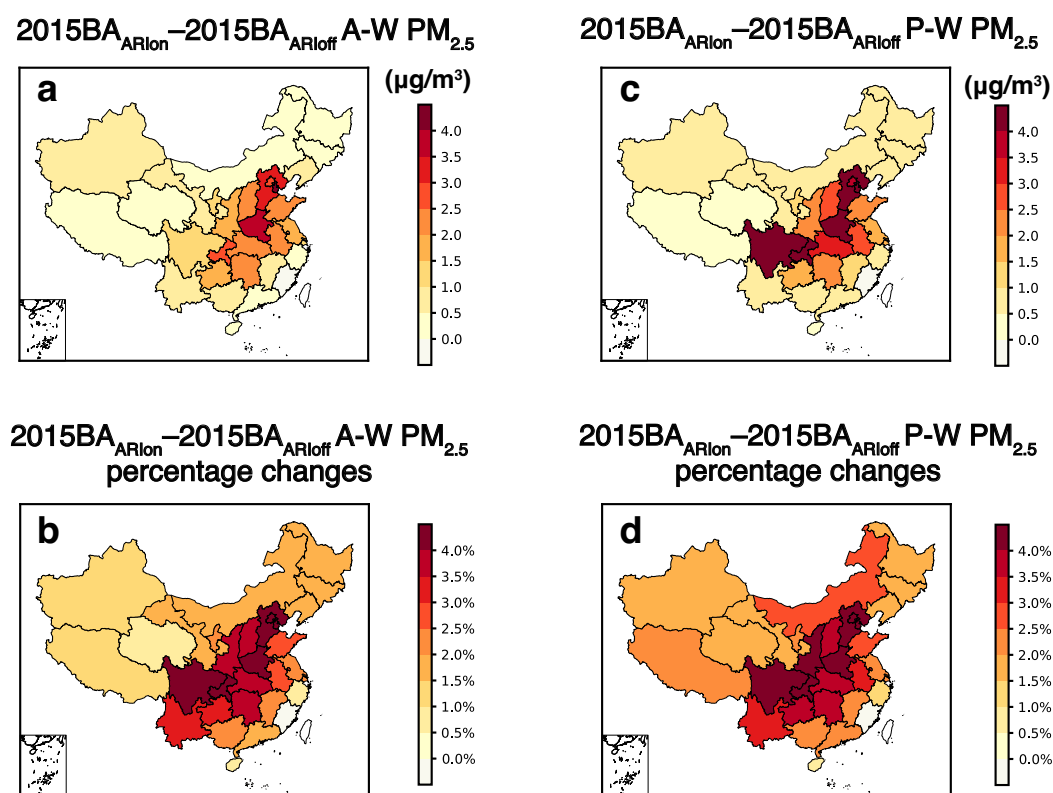
Extended data is available for this paper at <https://doi.org/10.1038/s41561-024-01425-1>.

Supplementary information The online version contains supplementary material available at <https://doi.org/10.1038/s41561-024-01425-1>.

Correspondence and requests for materials should be addressed to Yue Qin or Xin Huang.

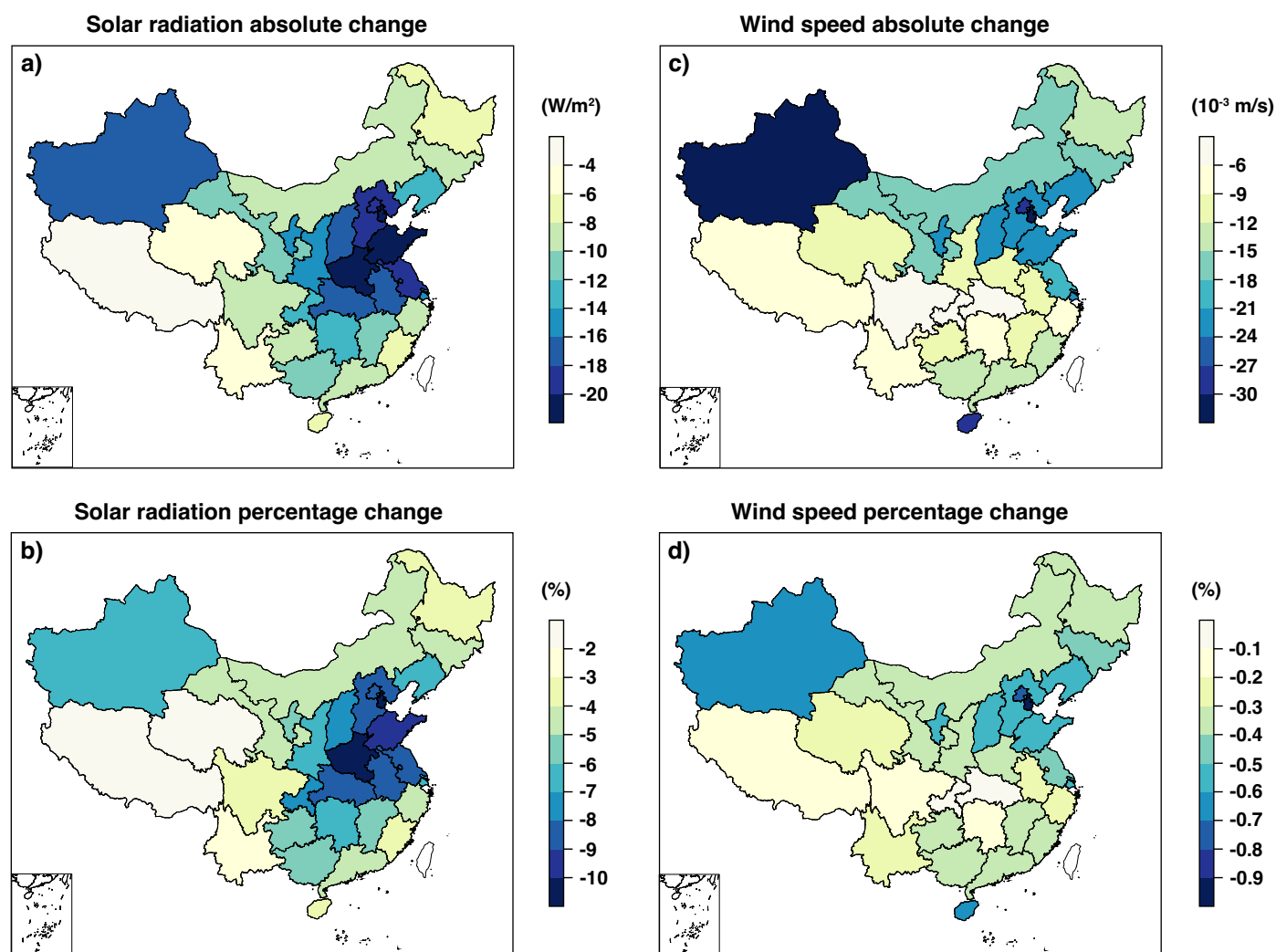
Peer review information *Nature Geoscience* thanks Jinyue Yan and the other, anonymous, reviewer(s) for their contribution to the peer review of this work. Primary Handling Editor: Xujia Jiang, in collaboration with the *Nature Geoscience* team.

Reprints and permissions information is available at www.nature.com/reprints.



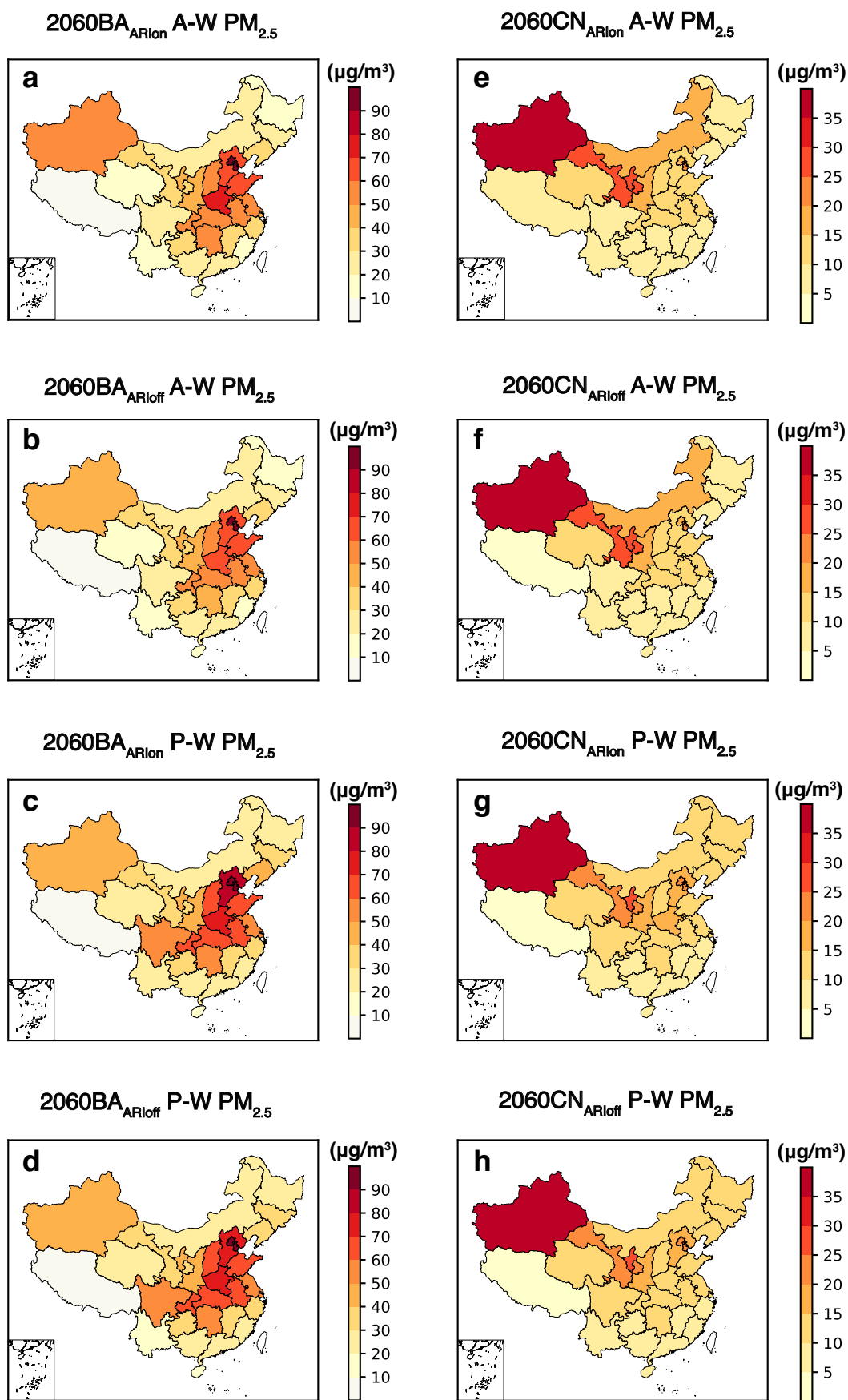
Extended Data Fig. 1 | Provincial PM_{2.5} surface concentration changes due to aerosols' radiative effects across mainland China in 2015. (a, b) Area-weighted (A-W) and (c, d) population-weighted (P-W) PM_{2.5} surface concentration changes in (a, c) absolute and (b, d) percentage changes across mainland China due to

aerosols' radiation interactions (ARI) in 2015. Base map data are from the Resource and Environment Science and Data Center, Institute of Geographic Sciences and Natural Resources Research, Chinese Academy of Sciences (<https://doi.org/10.12078/2023010103>, 2023)¹.



Extended Data Fig. 2 | Provincial solar radiation and wind speed changes due to aerosols' radiative effects across mainland China in 2015. (a, b) Solar radiation and (c, d) wind speed changes in (a, c) absolute and (b, d) percentage changes across mainland China. Base map data are from the Resource and

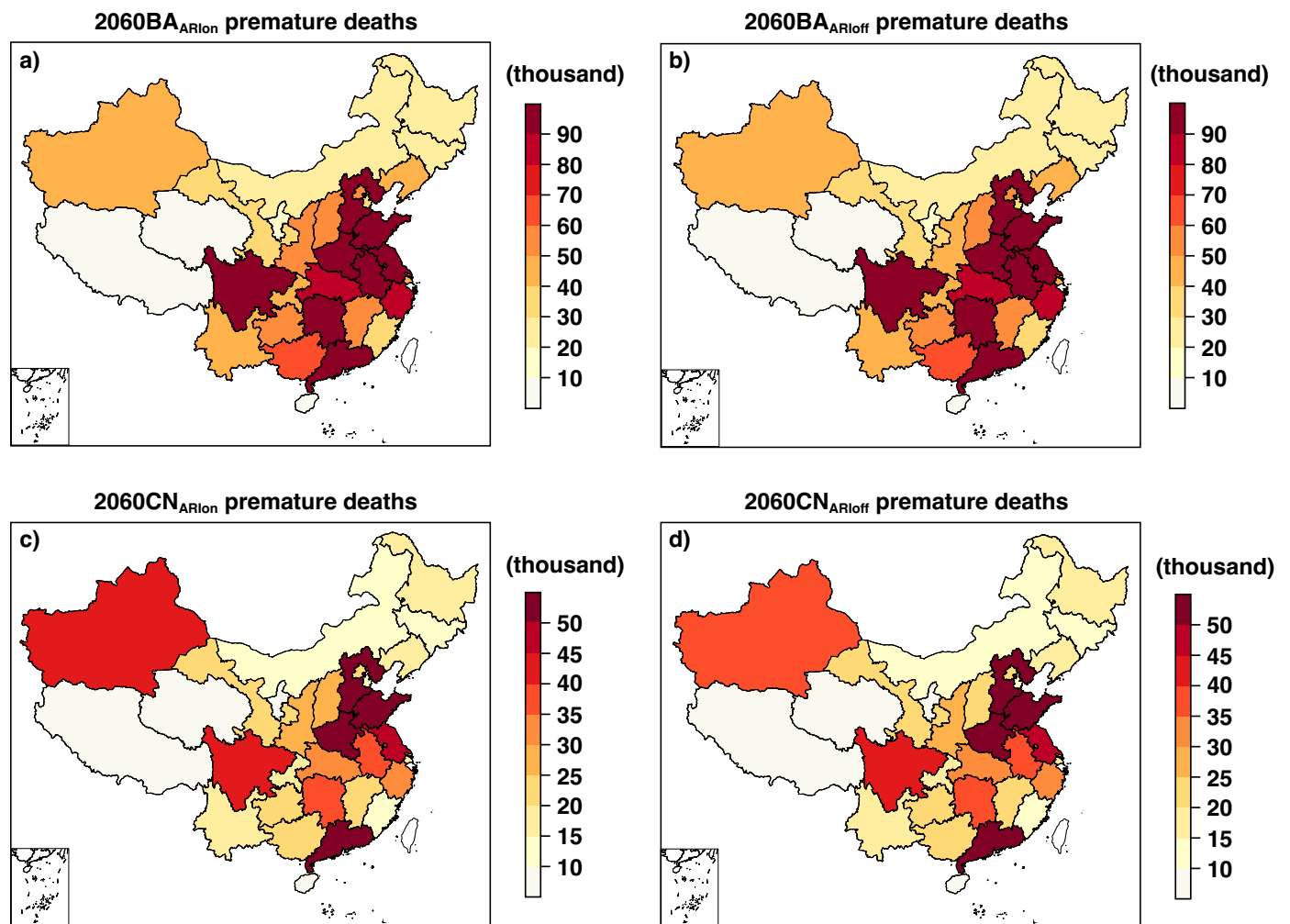
Environment Science and Data Center, Institute of Geographic Sciences and Natural Resources Research, Chinese Academy of Sciences (<https://doi.org/10.12078/2023010103>, 2023)¹.



Extended Data Fig. 3 | See next page for caption.

Extended Data Fig. 3 | 2060 Provincial PM_{2.5} surface concentrations in mainland China. Area-weighted (A-W) and population-weighted (P-W) PM_{2.5} surface concentration in **(a-d)** 2060 Baseline scenario and **(e-h)** 2060 Carbon neutral scenario, with (ARlon) and without (ARloff) considering aerosols'

radiation interactions respectively. Base map data are from the Resource and Environment Science and Data Center, Institute of Geographic Sciences and Natural Resources Research, Chinese Academy of Sciences (<https://doi.org/10.12078/2023010103>, 2023)¹.



Extended Data Fig. 4 | 2060 Provincial PM_{2.5} associated premature deaths in mainland China. PM_{2.5} associated premature deaths in (a,b) 2060 Baseline scenario, (c,d) 2060 Carbon neutral scenario with (ARI_{on}) and without (ARI_{off}) considering aerosols' radiation interactions respectively. Base map data are from

the Resource and Environment Science and Data Center, Institute of Geographic Sciences and Natural Resources Research, Chinese Academy of Sciences (<https://doi.org/10.12078/2023010103>, 2023)¹.

Extended Data Table. 1 | Scenarios design and description

Scenarios	Description
2015 Baseline (2015BA _{ARIon})	Lax climate and air pollution policy following a highly inequal and isolated socioeconom pathway in 2015
2015 Baseline-NoARI (2015BA _{ARIoff})	Same as 2015 Baseline while does not consider aerosol-radiation interactions
2060 Baseline (2060BA _{ARIon})	Lax climate and air pollution policy following a highly inequal and isolated socioeconom pathway in 2060
2060 Baseline-NoARI (2060BA _{ARIoff})	Same as 2060 Baseline while does not consider aerosol-radiation interactions
2060 Carbon Neutral (2060CN _{ARIon})	Realizing China's carbon neutral commitment combined with the best available end-of-pipe control technologies in 2060
2060 Carbon Neutral-NoARI (2060CN _{ARIoff})	Same as 2060 Carbon Neutral while does not consider aerosol-radiation interactions
2060 Carbon Neutral-2060Met (2060MET _{ARIon})	Same as 2060 Carbon Neutral while using future meteorology
2060 Carbon Neutral-NoARI-2060Met (2060MET _{ARIoff})	Same as 2060 Carbon Neutral-2060Met while does not consider aerosol-radiation interactions

¹Except for the 2060Met scenarios, fixed 2015 meteorology is used for all scenarios to isolate the impacts of emission changes and aerosols' radiative effects.

Scenarios design and description.